Journal of AI and Data Mining
Vol 6, No 1, 2018, 121-132

Multi-Output Adaptive Neuro-Fuzzy Inference System for Prediction of Dissolved Metal Levels in Acid Rock Drainage: a Case Study

H. Fattahi *, A. Agah and N. Soleimanpourmoghadam

Department of Mining Engineering, Arak University of Technology, Arak, Iran.

Received 07 February 2016; Revised 05 March 2017; Accepted 27 June 2017
Corresponding author: H.fattahi@arakut.ac.ir (H. Fattahi).

Abstract
Pyrite oxidation, Acid Rock Drainage (ARD) generation, and associated release and transport of toxic metals are a major environmental concern for the mining industry. Estimation of the metal loading in ARD is a major task in developing an appropriate remediation strategy. In this work, an expert system, the Multi-Output Adaptive Neuro-Fuzzy Inference System (MANFIS), is used for estimation of metal concentrations in the Shur River, resulting from ARD at the Sarcheshmeh porphyry copper deposit, SE of Iran. Concentrations of Cu, Fe, Mn, and Zn are predicted using the pH, and the sulfate (SO_4) and magnesium (Mg) concentrations in the Shur River as inputs to MANFIS. Three MANFIS models are implemented, Grid Partitioning (GP), Subtractive Clustering Method (SCM), and Fuzzy C-Means Clustering Method (FCM). A comparison is made between these three models, and the results obtained show the superiority of the MANFIS-SCM model. These results indicate that the MANFIS-SCM model has a potential for estimation of the metals with a high degree of accuracy and robustness.

Keywords: *Acid Rock Drainage, MANFIS, Grid Partitioning, Subtractive Clustering Method, Fuzzy C-Means Clustering Method.*

1. Introduction

The Sarcheshmeh copper mine is located in the Central Iranian Volcanic Belt in Kerman Province, SE of Iran [1,2]. The mine and mineral processing operation produces large tonnages of low-grade wastes and tailings materials that can generate Acid Rock Drainage (ARD) [3,4]. The waste and tailings materials contain reactive sulfide minerals, in particular pyrite, and have a short lag time before generating ARD. The mine generated acidic waters have high concentrations of dissolved iron and sulfate, a low pH (2-4.5), and variable concentrations of other elements, principally Mn, Zn, Cu, Cd, and Pb [5-9]. ARD containing metals threaten the aquatic life and surrounding environment [10-14]. The prediction of metal loadings to the Shur River is required to help develop effective mitigation strategies to minimize impacts to the river.

The Sarcheshmeh copper mine provides an excellent opportunity to investigate the processes involved in sulfide mineral oxidation and ARD generation within sulfide-bearing waste and tailings, and the impact of ARD on the Shur Rivers [15,16,2]. Numerous works have been done on different aspects of ARD at Sarcheshmeh and other mines in Iran including those outlined as what follow. Ardejani et al. [17] have offered a combined mathematical-geophysical model for prediction of pyrite oxidation. Sadeghi et al. [14] have investigated an image processing method applied to model the pyrite oxidation in the wastes of the AlborzSharghi coal washing plant, NE of Iran. Shokri et al. [18] have presented a statistical model for predicting pyrite oxidation in a coal waste pile at AlborzSharghi, Iran. Khorasanipour, Eslami [19] have investigated hydro-geochemistry and contamination by trace elements in Cu-Porphyry Mine tailings.

In the past few decades, the intelligent system approaches have gained increasing popularity in different fields of engineering for modeling and simulation of environmental problems. Kemper, Sommer [20] have estimated the metal concentrations in soils using a back propagation

network and multiple linear regression. Almasri, Kaluarachchi [21] have applied modular neural networks to predict the nitrate distribution in ground water using on-ground nitrogen loading and recharge data. Back-propagation neural network and multiple linear regression were used for prediction of water quality in the Gomti River in India [22]. Tahmasebi, Hezarkhani [23] have investigated the application of an Adaptive Neuro-Fuzzy Inference System (ANFIS) for grade estimation at the Sarcheshmeh Porphyry Copper Deposit. Gholami et al. [24] have used artificial intelligence methods for prediction of nickel mobilization. Rooki et al. [25] have applied neural networks for prediction of metals in acid mine drainage. Doulati Ardejanii et al. [4]have used the general regression neural network analysis for prediction of rare earth elements in neutral alkaline mine drainage from the Razi Coal Mine, Golestan Province, NE of Iran. Sadeghiamirshahidi et al. [26] have applied artificial neural networks (ANNs) for prediction of pyrite oxidation in the spoil of the AlborzSharghi coal washing refuse pile, NE of Iran. Sayadi et al. [27] have investigated the application of neural networks to predict the net present value in mining projects. Shokri et al. [28] have applied ANNs and ANFISs for prediction of pyrite oxidation in a coal washing waste pile in Iran. Maiti, Tiwari [29] have compared Bayesian neural networks and an ANFIS in groundwater level prediction.

The literature investigated has shown that many research works have been conducted related to the application of the ANN method in mining and relevant environmental problems.

In this work, the three MANFIS models MANFIS-GP, MANFIS-SCM, MANFIS-FCM were used to build the prediction models for the estimation of the ARD-derived metals in the Shur River.

The results obtained from the estimation using MANFIS were compared with the measured concentrations of the major metals in the Shur River.

2. Site descriptions

The Sarcheshmeh open pit copper mine is located 160 km SW of Kerman and 50 km to SW of Rafsanjan in the Kerman province, Iran (Figure 1); the main access road to the studied area is the Kerman–Rafsanjan–Shahr Babak road [30].

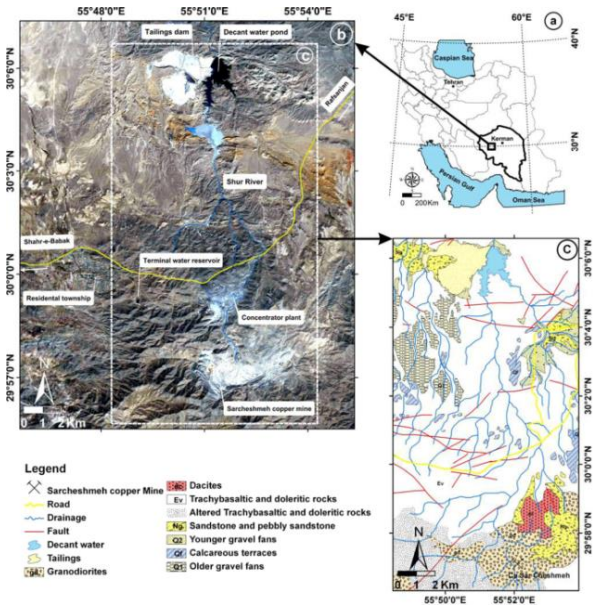

Figure 1. (a) Location of Kerman province, (b) satellite image, illustrating geographical situation of Sarcheshmeh copper complex, (c) geological map of studied area [31].

The ore body is recognized to be the fourth largest porphyry copper deposit in the world consisting of 1 billion tons of ore with copper (0.9%) and molybdenum (0.03%) [32]. The mine is situated in the rugged topography of the Band Mamazar-Pariz Mountains at an average elevation of 1,600 m. The mean annual precipitation at the site varies from 300 to 550 mm, the temperature ranges from +35 ^{o}C in summer to -20 ^{o}C in winter, and the area is covered with snow about 3–4 months per year [15,25]. The Sarcheshmeh ore body is oval-shaped with a width of about 1,200 m and a length of about 2,300 m. This deposit is centred on the late Tertiary Sarcheshmeh grano-diorite porphyry stock [33]. The geology of Sarcheshmeh porphyry deposit consists of a very complex series of magmatically related intrusives of Tertiary volcanic emplaced at variable distances from the edge of an older near-batholith-size granodiorite mass. The open pit mining method is used to extract the ore, the tailings impoundment is located about 20 km downstream of the open pit on the Shur River. The Shur River is the main recipient of the mine drainage including the ARD and industrial effluent of the Sarcheshmeh copper complex that discharges into the tailings impoundment [31]. The Shur River basin at the tailings dam site has a catchment area of approximately 200 km^2 and has a mean annual discharge of about 0.53 m^3/s [34].

3. Sampling and field methods

Water sampling was conducted in February

2006. In this work, 6 stations at different distances along the river between the mine and the tailings dam were selected for collecting the samples for water quality analysis.

The water samples were immediately acidified by adding HNO (10 cc acid to 1,000 cc sample) and stored under cool conditions [24]. THE Water sampling equipment included sterile sample containers, GPS, oven, autoclave, Ph-meter, and atomic adsorption and ICP analyzers. The pH values for the water samples were measured using a portable pH-meter in the field. Other quantities measured in the field included electrical conductivity (EC), total dissolved solids (TDS), and temperature. Analyses of the dissolved metals were performed using an adsorption spectrometer (AA220) in the water laboratory of the National Iranian Copper Industries Company (NICIC). The ICP (model 6000) analysis was used to analyze the concentrations of those metals, usually detected in the range of ppb [35,36].

4. Multi-Output Adaptive Neuro-Fuzzy Inference System

ANN is simple but a powerful and flexible tool for forecasting, provided that there is enough data for training, an adequate selection of the input–output samples, an appropriated number of hidden units, and enough computational resources available. Also ANN has the well-known advantages of being able to approximate any non-linear function and being able to solve problems where the input–output relationship is neither well-defined nor easily computable because ANN is data-driven. Multi-layered feed-forward ANN is specially suited for forecasting, implementing non-linearities using sigmoid functions for the hidden layer and linear functions for the output layer [37].

Just like ANN, a fuzzy logic system is a non-linear mapping of an input vector into a scalar output but it can handle numerical values and linguistic knowledge. In general, a fuzzy logic system contains four components: fuzzifier, rules, inference engine, and defuzzifier. The fuzzifier converts a crisp input variable into a fuzzy representation, where membership functions give the degree of belonging of the variable to a given attribute. Fuzzy rules are of the type ‘‘if–then’’, and can be derived from numerical data or from expert linguistic. The Mamdani and Sugeno inference engines are two of the main types of inference mechanisms. The Mamdani engine combines the fuzzy rules into a mapping from fuzzy input sets to fuzzy output sets, while the Takagi–Sugeno type relates fuzzy inputs and crisp outputs. The defuzzifier converts a fuzzy set into a crisp number using the centroid of area, bisector of area, mean of maxima or maximum criteria [38,39].

ANN has the advantage over the fuzzy logic models that knowledge is automatically acquired during the learning process. However, this knowledge cannot be extracted from the trained network behaving as a black box. Fuzzy systems, on the other hand, can be understood through their rules but these rules are difficult to define when the system has too many variables and their relations are complex [40].

A combination of ANN and fuzzy systems has the advantages of each of them. In a neuro-fuzzy system, neural networks extract automatically fuzzy rules from numerical data and, through the learning process, the membership functions are adaptively adjusted. ANFIS is a class of adaptive multi-layer feed-forward networks, applied to non-linear forecasting where past samples are used to forecast the sample ahead. ANFIS incorporates the self-learning ability of ANN with the linguistic expression function of fuzzy inference [41].

The ANFIS network [42] is composed of five layers:

Layer 1: each node i in this layer generates a membership grades of a linguistic label. For instance, the node function of the i^{th} node might be:

$$Q_i^1 = \mu_{A_i}(x) = \frac{1}{1+\left[\left(\frac{x-v_i}{\sigma_i}\right)^2\right]^{b_i}} \quad (1)$$

where, x is the input to node i, μ is the membership functions of the MANFIS system, and A_i is the linguistic label (small, large, …) associated with this node; and $\{\sigma_i, v_i, b_i\}$ is the parameter set that changes the shapes of the membership function. Parameters in this layer are referred to as the "premise parameters".

Layer 2: Each node in this layer calculates the "firing strength" of each rule via multiplication:

$$Q_i^2 = W_i = \mu_{Ai}(x).\mu_{Bi}(y) \qquad i = 1,2 \quad (2)$$

The firing strength of a rule is given by the product of the input membership grades, and this value is passed to the membership grade of the output to the corresponding fuzzy set.

W_i is The weight of the layer 2, μ_{Ai} and μ_{Bi} are symbols for membership functions of the inputs x and y, respectively.

Layer 3: The i^{th} node of this layer calculates the ratio of the i^{th} rule's firing strength to the sum of all rules' firing strengths:

$$Q_i^3 = \bar{W}_i = \frac{w_i}{\sum_{j=1}^{2} w_j}, \quad i = 1,2 \tag{3}$$

$\bar{W}_i$ is normalized weights of the layer 3. For convenience, outputs of this layer will be called "normalized firing" strengths.

Layer 4: Every node i in this layer is a node function:

$$Q_i^4 = \bar{W}_i f_i = \bar{W}_i (p_i x + q_i y + r_i) \tag{4}$$

where, $\bar{W}_i$ is the output of layer 3. Parameters in this layer will be referred to as "consequent parameters".

Each node in this layer is an adaptive node. Its output is obtained by multiplying the corresponding weight of the layer 3 in a first-order polynomial that is defined as the output membership function.

Layer 5: The overall output is determined by summation of all incoming signals of the layer 4.

$$Q_i^5 = Overall\ Output = \sum \bar{W}_i f_i = \frac{\sum w_i f_i}{\sum w_i} \tag{5}$$

The MANFIS used in this paper possesses a similar architecture to a classic ANFIS system, except for a difference in the fourth layer [43,44]. The difference is the increase in the number of weights of the multi-output neuro-fuzzy system that allows improving the precision of approximation. Design of the MANFIS system for three outputs and one-input is shown in figure 2, and the system logic is described below [45].

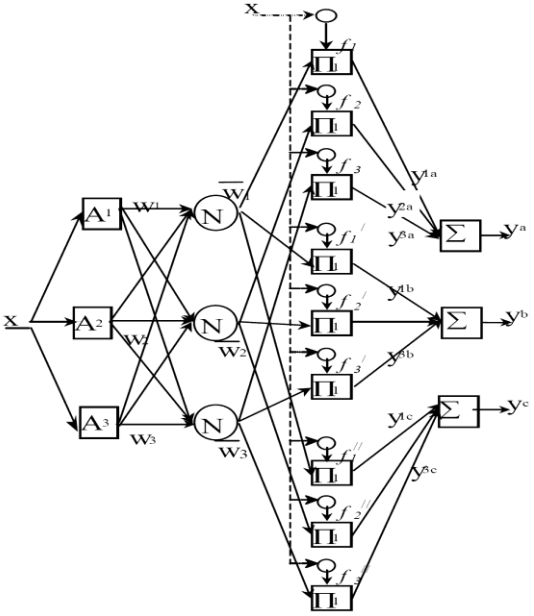

Figure 2. Architecture of MANFIS system for three outputs and one-input [45].

The following is a layer-by-layer description of a one-input one-rule first-order Sugeno system [46,43]

Layer 1: Generates the membership grades:

$$o_i^1 = g(x) \tag{6}$$

g: the membership function of the MANFIS system.

Layer 2: Generates the firing strengths:

$$o_i^2 = w_i = \prod_{j=1}^{m} g(x) \tag{7}$$

Layer 3: Normalizes the firing strengths:

$$o_i^3 = \bar{w}_i = \frac{w_i}{w_i + w_2 + w_3} \tag{8}$$

Layer 4: Calculates rule outputs based on the consequent parameters:

$$o_i^4 = y_i = \bar{w}_i . \mathrm{f}_i = \bar{w}_i . (\mathrm{p}_i . x + q_i . x + r_i) \tag{9}$$

$$o_i^{4'} = y_i' = \bar{w}_i . \mathrm{f}_i' = \bar{w}_i . (\mathrm{p}_i' . x + q_i' . x + r_i')$$

$$o_i^{4''} = y_i'' = \bar{w}_i . \mathrm{f}_i'' = \bar{w}_i . (\mathrm{p}_i'' . x + q_i'' . x + r_i'')$$

Layer 5: Sums all the inputs from layer 4:

$$o_i^5 = y_a = \sum_{i=1}^{n} y_i = \sum_{i=1}^{n} \bar{w}_i . \mathrm{f}_i = \bar{w}_i . (\mathrm{p}_i . x + q_i . x + r_i) \tag{10}$$

$$o_i^{5'} = y_b = \sum_{i=1}^{n} y_i' = \sum_{i=1}^{n} \bar{w}_i . \mathrm{f}_i' = \bar{w}_i . (\mathrm{p}_i' . x + q_i' . x + r_i')$$

$$o_i^{5''} = y_c = \sum_{i=1}^{n} y_i'' = \sum_{i=1}^{n} \bar{w}_i . \mathrm{f}_i'' = \bar{w}_i . (\mathrm{p}_i'' . x + q_i'' . x + r_i'')$$

For a given dataset, different MANFIS models can be constructed using different identification methods. Grid partitioning, subtractive clustering method, and fuzzy C-means clustering method are the three methods used in this paper to identify the antecedent membership functions. These methods are described below.

4.1. Grid Partitioning of the Antecedent Variables

This method proposes the dependent partitions of each antecedent variable [43]. The expert developing the model can define the membership functions of all antecedent variables using prior knowledge and experience. They are designed to represent the meaning of the linguistic terms in a given context. However, for many systems, no specific knowledge is available on these partitions. In that case, the domains of the antecedent variables can simply be partitioned into a number of equally spaced and equally shaped membership functions [47]. Therefore, in the grid partitioning method, the domain of each antecedent variable is partitioned into equidistant and identically shaped membership functions. Using the available input-output data, the

parameters of the membership functions can be optimized.

4.2. Subtractive Clustering method

The subtractive clustering method proposed by Chiu [48] considers the data points as the candidates for the center of clusters. The algorithm is developed as follows:

At first, a collection of n data points $\{X_1, X_2, X_3, ..., X_n\}$ in an M-dimensional space is considered. Since each data point is a candidate for a cluster center, a density measure at data point X_i is defined as:

$$D_i = \sum_{j=1}^{n} \exp\left(-\frac{\left\| x_i - x_j \right\|^2}{\left(\frac{r_a}{2} \right)^2} \right) \quad (11)$$

where, r_a is a positive constant. Hence, a data point will have a high density value if it has many neighboring data points. The radius r_a defines a neighborhood; data points outside this radius contribute only slightly to the density measure. After the density measure of each data point has been calculated, the data point with the highest density measure is selected as the first cluster center. Let X_{c1} be the point selected and D_{c1} be its density measure. Next, the density measure for each data point x_i is revised as follows:

$$D_i = D_i - D_{ci} \exp\left(-\frac{\left\| x_i - x_{ci} \right\|^2}{\left(\frac{r_b}{2} \right)^2} \right) \quad (12)$$

where, r_b is a positive constant. After the density calculation for each data point is revised, the next cluster center X_{c2} is selected and all the density calculations for data points are revised again. This process is repeated until a sufficient number of cluster centers are generated.

SCM is an attractive approach to the synthesis of the MANFIS networks, which estimates the cluster number and its cluster location automatically. In the subtractive clustering algorithm, each sample point is seen as a potential cluster center. Using this method, the computation time becomes linearly proportional to data size but independent from the dimension of the problem under consideration [49-56]. Using SCM, the cluster center of all data can be found. Then the number of subtractive centers is used to generate automatic membership functions and rule base as well as the location of the membership function within dimensions.

4.3. Fuzzy C-means Clustering method

Fuzzy C-means Clustering Method is a data clustering algorithm proposed by [Bezdek [57]], in which each data point belongs to a cluster to a degree specified by a membership grade. FCM partitions a collection of n vectors X_i, $i = 1, 2, ..., n$, into C fuzzy groups, and finds a cluster center in each group such that a cost function of dissimilarity is minimized. The stages of the FCM algorithm are described in brief in the following text. First, the cluster centers c_i, $i = 1, 2, ..., C$ are chosen randomly from the n points $\{X_1, X_2, X_3, ..., X_n\}$. After that, the membership matrix U is computed using the following equation:

$$\mu_{ij} = \frac{1}{\sum_{k=1}^{c} \left(\frac{d_{ij}}{d_{kj}} \right)^{2/m-1}} \quad (13)$$

where, $d_{ij} = \left\| c_i - x_j \right\|$ is the Euclidean distance between the i^{th} cluster center and the j^{th} data point, and m is the fuzziness index. Then the cost function is computed according to the following equation [58]. The process is stopped if it is below a certain threshold.

$$J(U, c_1, ..., c_2) = \sum_{i=1}^{c} J_i = \sum_{i=1}^{c} . \sum_{j=1}^{n} \mu_{ij}^m d_{ij}^2 \quad (14)$$

In the final step, the new c fuzzy cluster centers c_i, $i = 1, 2, ..., C$ are computed using the following equation:

$$c_i = \frac{\sum_{j=1}^{n} \mu_{ij}^m x_j}{\sum_{j=1}^{n} \mu_{ij}^m} \quad (15)$$

5. Prediction of Metals in Acid Rock Drainage using, MANFIS model

In this work, MANFIS was used to build a prediction model for estimation of metal concentration in ARD of Sarcheshmeh porphyry copper deposit using MATLAB. Three MANFIS techniques were implemented, namely: GP, SCM and FCM. Figure 3 shows the fuzzy architecture of the MANFIS. As it can be seen in figure 3, pH, SO_4, and Mg were introduced as the input parameters into the MANFIS models, and Cu, Fe, Mn, Zn as the outputs. Part of the dataset used in this work is presented in table 1. Also descriptive statistics of the all datasets are shown in table 2.

Figure 3. Architecture of MANFIS based on GP, SCM, and FCM.

Table 1. Part of dataset used in this work (concentrations of elements are given in ppm).

	Inputs			Outputs			
	PH	SO_4	Mg	Cu	Fe	Mn	Zn
Training data set	3.91	1100	78.2	69.8	0.65	49.6	15.3
	3.84	798	60.77	46.5	3.42	27.7	10.07
	4.85	770	30.48	16	2.68	20.4	8.69
	5.54	1005	51.75	3.79	7.77	12.79	4.55
	5.46	775	58.3	0.31	0.21	10.9	3.42
	5.56	698	54.29	0.899	4.065	9.52	2.8
	5.52	765	62.87	1.06	2.5	8.51	3.07
	5.8	540	40.67	0.02	8.26	7.08	7.53
	6.6	284	42	0.01	0.3	4.2	0.05
	7.2	249	34.5	0.01	0.01	0.04	0.01
Testing dataset	5.5	737	13	15	14	12	7.5
	6	650	50	13	2	15	0
	5.5	650	50	28	4	16	6
	6.2	750	50	23	2.5	16	5.6
	5.61	790	66.8	8	4	11.5	4

Table 2. Statistical description of 55 datasets used for construction of model (concentrations of elements are given in ppm).

Parameter	Min	Max	Average	Standard deviation
PH	3.3	7.2	5.34	1.01
SO4	27	1526	778.45	274.31
Mg	13	123	56.704	21.28
Cu	0	158	20.29	30.40
Fe	0.01	23	4.60	4.36
Mn	0.04	52	16.05	11.49
Zn	0	31.48	6.32	5.49

5.1. Pre-processing of data

In data-driven system modeling methods, some pre-processing steps are usually implemented prior to any calculations in order to eliminate outliers, missing values or bad data. This step ensures that the raw data retrieved from the database is suitable for modeling. In order to soften the training procedure and improve the accuracy of prediction, the data samples were normalized to the interval [0, 1] according to the following linear mapping function:

$$x_M = \frac{x - x_{\min}}{x_{\max} - x_{\min}} \tag{16}$$

where, m x is the original value from the dataset, x_M is the mapped value, and x_{min} (x_{max}) denotes the minimum (maximum) raw input values, respectively.

The model outputs are remapped to their corresponding real values by the inverse mapping function ahead of calculating performance criterion.

5.2. Performance criteria

In order to evaluate the performance of the MANFIS models, the mean squared error (MSE) and squared correlation coefficient (R^2) tests were chosen to be the measure of accuracy. Let y_i be the actual value and $\hat{y}_i$ be the predicted value of the i^{th} observation, and n be the number of samples. The higher the R^2, the better is the model performance. For instance, an R^2 of 100% means that the measured output has been predicted exactly (perfect model).

$R^2 = 0$ means that the model performs as poorly as a predictor using simply the mean value of the data. Also a lower MSE indicates better performance of the model. MSE and R^2 are defined, respectively, as follow:

$$MSE = \frac{1}{n}\sum_{i=1}^{n}(y_i - \hat{y}_i)^2 \tag{17}$$

$$R^2 = 1 - \frac{\sum_{i=1}^{n}(y_i - \hat{y}_i)^2}{\sum_{i=1}^{n} y_i^2 - \frac{\sum_{i=1}^{n}\hat{y}_i^2}{n}} \tag{18}$$

6. Results and discussion

The training and testing procedures of the three MANFIS models (GP, SCM, FCM) were conducted. A dataset that included 55 data points was employed in the current work, while 44 data points (80%) were utilized for constructing the model and the remainder data points (11 data points) were utilized for assessment of degree of accuracy and robustness.

The MSE and R^2 values obtained for training datasets indicate the capability of learning the structure of data samples, whereas the results of testing dataset reveal the generalization potential and the robustness of the system modeling methods. The characteristics of the MANFIS models are presented in table 3.

Table 3. Characteristics of MANFIS models.

MANFIS parameter	MANFIS (GP)	MANFIS (SCM)	MANFIS (FCM)
Membership function type	Gaussian	Gaussian	Gaussian
Output membership function	Linear	Linear	Linear
Number of nodes	286	310	166
Number of linear parameters	500	152	80
Number of nonlinear parameters	30	228	120
Total number of parameters	530	380	200
Number of training data pairs	44	44	44
Number of testing data pairs	11	11	11
Number of fuzzy rules	125	38	20

The number of fuzzy rules obtained for the GP, SCM, and FCM models are 125, 38 and 20, respectively. The membership functions of the input parameters for different models are shown in figures 4-6.

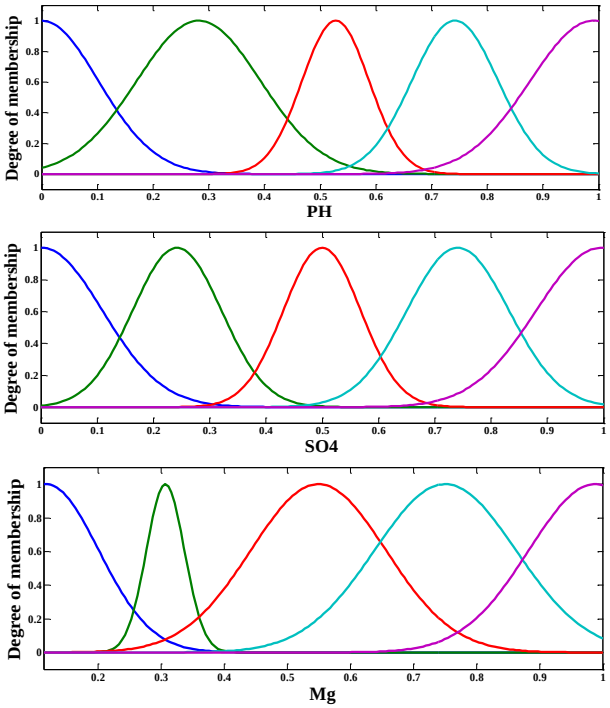

Figure 4. Membership functions obtained by MANFIS-GP model.

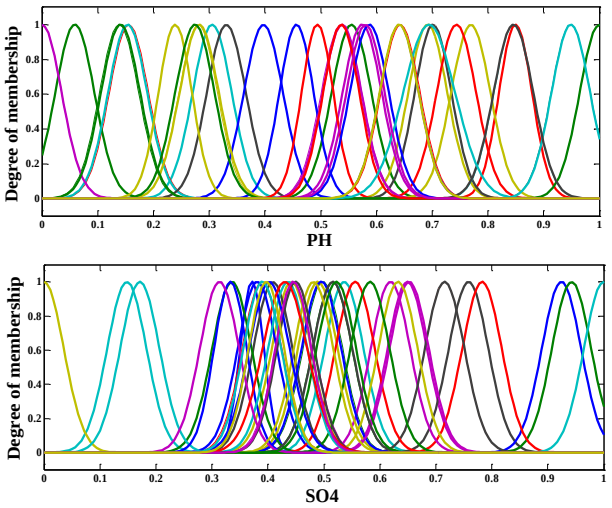

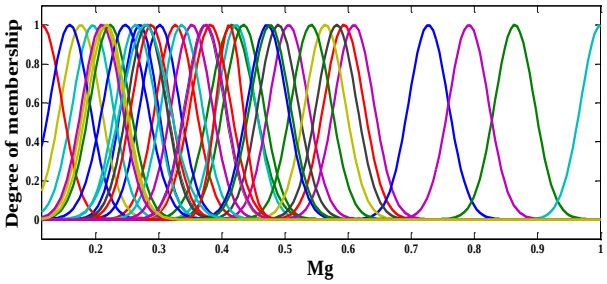

Figure 5. Membership functions obtained by MANFIS-SCM model.

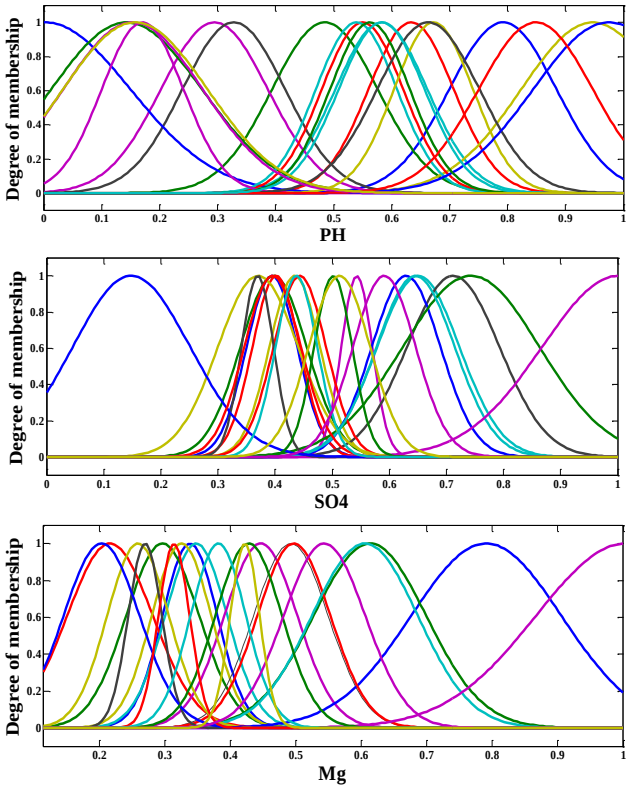

Figure 6 Membership functions obtained by MANFIS-FCM model.

In the MANFIS simulation, an expert is not required to establish the membership functions, the number of membership functions assigned to each input variable is chosen empirically by plotting the datasets and examining them visually or simply by trial and error. A comparison between the results obtained from the three models is shown in table 4. As it can be observed in this table, the MANFIS-SCM model performs better than the other two models for estimation of metals in the ARD of Sarcheshmeh porphyry copper deposit.

Correlation between the measured and predicted values of metals in ARD for testing phases is shown in figures 7-10.

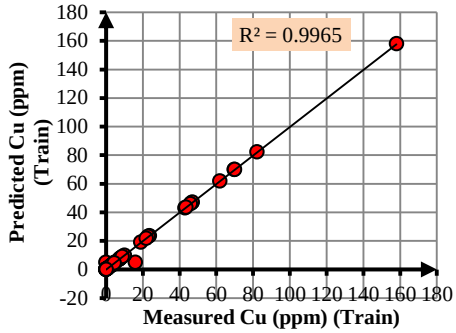

(a)

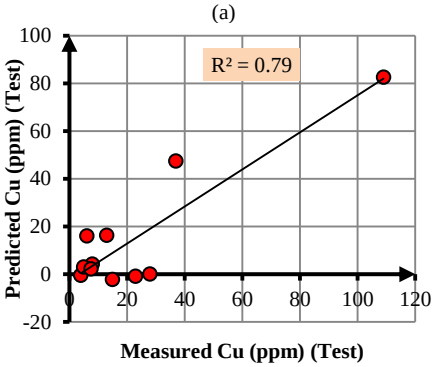

(b)

Figure 7. Correlation between measured and predicted values of Cu by MANFIS-SCM model a) training datasets, b) testing datasets.

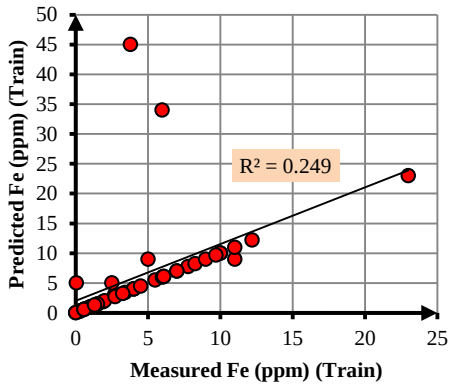

(a)

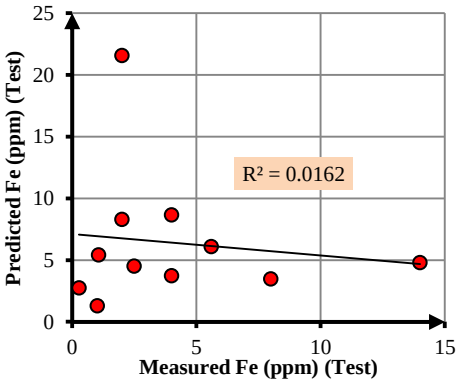

(b)

Figure 8. Correlation between measured and predicted values of Fe by MANFIS-SCM model a) training datasets, b) testing datasets.

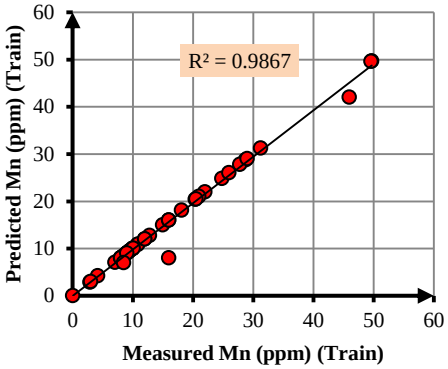

(a)

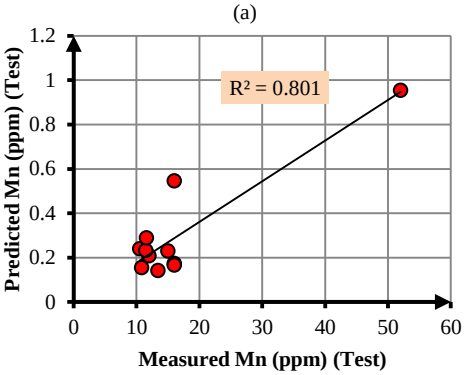

(b)

Figure 9. Correlation between measured and predicted values of Mn by MANFIS-SCM model a) training datasets, b) testing datasets.

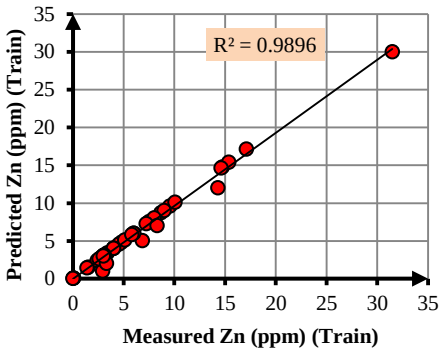

(a)

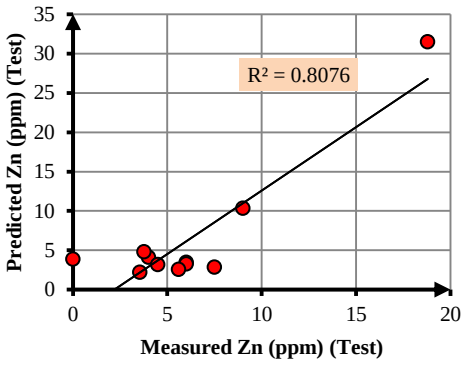

(b)

Figure 10. Correlation between measured and predicted values of Zn by MANFIS-SCM model a) training datasets, b) testing datasets

Table 4. A comparison between results of three models for testing datasets.

MANFIS model	Cu		Fe		Mn		Zn	
	MSE	R^2	MSE	R^2	MSE	R^2	MSE	R^2
MANFIS-GP	0.179	0.59	0.522	0.003	0.083	0.37	0.049	0.75
MANFIS-SCM	0.009	0.79	0.099	0.016	0.011	0.801	0.020	0.807
MANFIS-FCM	0.025	0.31	0.071	0.023	0.025	0.66	0.085	0.79

Also a comparison between the predicted values of metals in ARD by the MANFIS-SCM model and measured values is shown in figures 11-14.

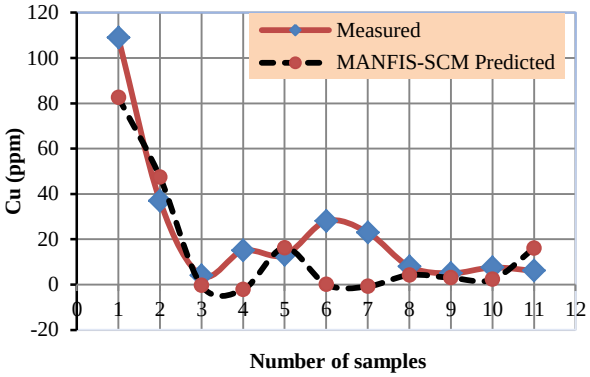

Figure 11. Comparison between measured and predicted Cu by MANFIS-SCM model for testing.

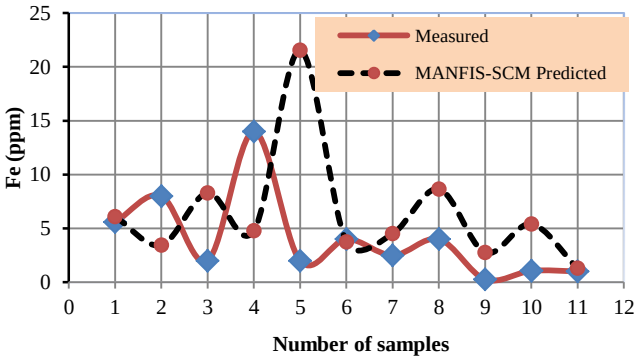

Figure 12. Comparison between measured and predicted Fe by MANFIS-SCM model for testing.

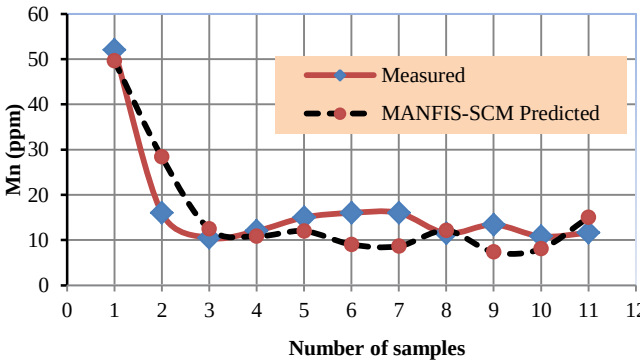

Figure 13. Comparison between measured and predicted Mn by MANFIS-SCM model for testing.

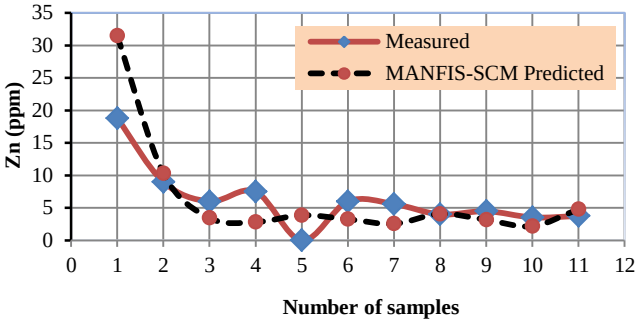

Figure 14. Comparison between measured and predicted Zn by MANFIS-SCM model for testing.

As shown in these figures, the results of the MANFIS-SCM model provided a good-fit to the measured values of Cu, Mn and Zn concentrations, and poor fit for Fe concentration. The poor-fit model for Fe ion is a result of the low correlation between Fe and the independent variables. The R^2 values for training stages of MANFIS-SCM were 0.99, 0.24, 0.98, and 0.98 for Cu, Fe, Mn and Zn, respectively. A comparison between the predicted concentrations and the measured data resulted in the correlation coefficients for testing stages of MANFIS-SCM, R^2, 0.79, 0.016, 0.80, and 0.80 for the Cu, Fe, Mn, and Zn ions respectively.

7. Conclusions

In a conventional fuzzy inference system, the number of rules is decided by an expert who is familiar with the target system to be modeled. The MANFIS method results in a better performance than the other intelligent methods due to the combination of FL and ANN. In a MANFIS simulation, however, no expert is required, and the number of membership functions (MFs) assigned to each input variable is chosen empirically, i.e. by plotting the datasets and examining them visually or simply by trial and error. For datasets with more than three inputs and two outputs, visualization techniques are not very effective and most of the time trial and error must be relied on.

Consequently, an automatic model identification method becomes a must, which is often realized by means of a training set of input-output pairs. In this paper, a new method to predict major metals (Cu, Fe, Mn and Zn) in Shur River impacted by ARD has been presented using the MANFIS method using 55 data samples and the following are concluded:

- A comparison was made between three MANFIS models, GP, SCM, and FCM and based upon the performance indices; R^2 and

MSE, MANFIS-SCM model was shown to be the best predictive model.

- Consequently, it is concluded that MANFIS-SCM is a reliable system modeling technique for estimation of metals in the AMD of Sarcheshmeh porphyry copper deposit with a highly acceptable degree of accuracy and robustness.

References

[1] Malakooti, S. J., Tonkaboni, S. Z. S., Noaparast, M., Ardejani, F. D., & Naseh, R. (2014). Characterisation of the Sarcheshmeh copper mine tailings, Kerman province, southeast of Iran. Environmental earth sciences, vol. 71, pp. 2267-2291.

[2] Shahabpour, J., & Doorandish, M. (2008). Mine drainage water from the Sar Cheshmeh porphyry copper mine, Kerman, IR Iran. Environmental monitoring and assessment, vol. 141, pp. 105-120.

[3] Ardejania, F. D., Karamib, G. H., Assadib, A. B., & Dehghan, R. A. Hydrogeochemical investigations of the Shour River and groundwater affected by acid mine drainage in Sarcheshmeh porphyry copper mine. In: 10th International mine water association congress, 2008. pp 235-238.

[4] Doulati Ardejanii, F., Rooki, R., Jodieri Shokri, B., Eslam Kish, T., Aryafar, A., & Tourani, P. (2012). Prediction of rare earth elements in neutral alkaline mine drainage from Razi Coal Mine, Golestan Province, northeast Iran, using general regression neural network. Journal of Environmental Engineering, vol. 139, pp. 896-907.

[5] Williams, R. (1975). Waste production and disposal in mining, milling, and metallurgical industries. Miller-Freeman Publishing Company, San Francisco, pp. p 485.

[6] Chen, C., & Vachtsevanos, G. (2012). Bearing condition prediction considering uncertainty: An interval type-2 fuzzy neural network approach. Robotics and Computer-Integrated Manufacturing, vol. 28, pp. 509-516.

[7] Cánovas, C., Olías, M., Nieto, J., Sarmiento, A., & Cerón, J. (2007). Hydrogeochemical characteristics of the Tinto and Odiel Rivers (SW Spain). Factors controlling metal contents. Science of the Total Environment, vol. 373, pp. 363-382.

[8] Moncur, M., Ptacek, C., Blowes, D., & Jambor, J. (2005). Release, transport and attenuation of metals from an old tailings impoundment. Applied Geochemistry, vol. 20, pp. 639-659.

[9] Lottermoser, B. (2007). Mine wastes. Springer, Berlin, pp.

[10] Kim, Y., Mallick, R., Bhowmick, S., & Chen, B.-L. (2013). Nonlinear system identification of large-scale smart pavement systems. Expert Systems with Applications, vol. 40, pp. 3551-3560.

[11] Dinelli, E., Lucchini, F., Fabbri, M., & Cortecci, G. (2001). Metal distribution and environmental problems related to sulfide oxidation in the Libiola copper mine area (Ligurian Apennines, Italy). Journal of Geochemical Exploration, vol. 74, pp. 141-152.

[12] Lee, J., & Chon, H. (2006). Hydrogeochemical characteristics of acid mine drainage in the vicinity of an abandoned mine, Daduk Creek, Korea. Journal of Geochemical Exploration, vol. 88, pp. 37-40.

[13] Sahoo, P., Tripathy, S., Panigrahi, M., & Equeenuddin, S. M. (2014). Geochemical characterization of coal and waste rocks from a high sulfur bearing coalfield, India: Implication for acid and metal generation. Journal of Geochemical Exploration, vol. 145, pp. 135-147.

[14] Sadeghi, S., Rezvanian, A., & Kamrani, E. (2012). An efficient method for impulse noise reduction from images using fuzzy cellular automata. AEU-International Journal of Electronics and Communications, vol. 66, pp. 772-779.

[15] Ardejani, F. D., Karami, G., Assadi, A., & Dehghan, R. (2008). Hydrogeochemical investigations of the Shour River and groundwater affected by acid mine drainage in Sarcheshmeh porphyry copper mine. 10th international mine water association congress, Karlovy Vary, Czech Republic, pp. pp 235–238.

[16] Marandi, R., Doulati Ardejani, F., & Marandi, A. Biotreatment of acid mine drainage using sequencing batch reactors (SBRs) in the Sarcheshmeh porphyry copper mine. In: IMWA symposium, 2007. pp 221-225

[17] Ardejani, f. D., Shokri, B. J., Moradzadeh, A., Soleimani, e., & Jafari, M. A. (2008). A combined mathematical geophysical model for prediction of pyrite oxidation and pollutant leaching associated with a coal washing waste dump. International Journal of Environmental Science & Technology, vol. 5, pp. 517-526.

[18] Shokri, B. J., Ramazi, H., Ardejani, F. D., & Moradzadeh, A. (2014). A statistical model to relate pyrite oxidation and oxygen transport within a coal waste pile: case study, Alborz Sharghi, northeast of Iran. Environmental earth sciences, vol. 71, pp. 4693.

[19] Khorasanipour, M., & Eslami, A. (2014). Hydrogeochemistry and Contamination of Trace Elements in Cu-Porphyry Mine Tailings: A Case Study from the Sarcheshmeh Mine, SE Iran. Mine Water and the Environment, pp. 1-18.

[20] Kemper, T., & Sommer, S. (2002). Estimate of heavy metal contamination in soils after a mining accident using reflectance spectroscopy. Environmental science & technology, vol. 36, pp. 2742-2747.

[21] Almasri, M. N., & Kaluarachchi, J. J. (2005). Modular neural networks to predict the nitrate distribution in ground water using the on-ground nitrogen loading and recharge data. Environmental Modelling & Software, vol. 20, pp. 851-871.

[22] Singh, K. P., Basant, A., Malik, A., & Jain, G. (2009). Artificial neural network modeling of the river water quality—a case study. Ecological Modelling, vol. 220, pp. 888-895.

[23] Tahmasebi, P., & Hezarkhani, A. (2012). A hybrid neural networks-fuzzy logic-genetic algorithm for grade estimation. Computers & Geosciences, vol. 42, pp. 18-27.

[24] Gholami, R., Kamkar-Rouhani, A., Ardejani, F. D., & Maleki, S. (2011). Prediction of toxic metals concentration using artificial intelligence techniques. Appl Water Sci, pp. 125–134.

[25] Rooki, R., Doulati Ardejani, F., Aryafar, A., & Bani Asadi, A. (2011). Prediction of heavy metals in acid mine drainage using artificial neural network from the Shur River of the Sarcheshmeh porphyry copper mine, Southeast Iran. Environmental earth sciences, vol. 64, pp. 1303-1316.

[26] Sadeghiamirshahidi, M., Eslam kish, T., & Doulati Ardejani, F. (2013). Application of artificial neural networks to predict pyrite oxidation in a coal washing refuse pile. Fuel, vol. 104, pp. 163-169.

[27] Sayadi, A. R., Tavassoli, S. M. M., Monjezi, M., & Rezaei, M. (2014). Application of neural networks to predict net present value in mining projects. Arabian Journal of Geosciences, vol. 7, pp. 1067-1072.

[28] Shokri, B. J., Ardejani, F. D., Ramazi, H., & Sadeghiamirshahidi, M. (2014). Prediction of Pyrite Oxidation in a Coal Washing Waste Pile Applying Artificial Neural Networks (ANNs) and Adaptive Neuro-fuzzy Inference Systems (ANFIS). Mine Water and the Environment, pp. 146–156.

[29] Maiti, S., & Tiwari, R. K. (2014). A comparative study of artificial neural networks, Bayesian neural networks and adaptive neuro-fuzzy inference system in groundwater level prediction. Environmental Earth Sciences, vol. 71, pp. 3147-3160.

[30] Derakhshandeh, R., & Alipour, M. (2010). Remediation of acid mine drainage by using tailings decant water as a neutralization agent in Sarcheshmeh copper mine. Res J Environ Sci 4(3):, pp. 250–260.

[31] Jannesar Malakooti, S., Shahhosseini, M., Doulati Ardejani, F., Ziaeddin Shafaei Tonkaboni, S., & Noaparast, M. (2015). Hydrochemical characterisation of water quality in the Sarcheshmeh copper complex, SE Iran. Environmental Earth Sciences, vol. 74, pp. 3171-3190.

[32] Banisi, S., & Finch, J. (2001). Testing a floatation column at the Sarcheshmeh copper mine. Miner Eng 14(7):, pp. 785–789.

[33] Waterman, G. C., & Hamilton, R. (1975). The Sar Cheshmeh porphyry copper deposit. Economic Geology, vol. 70, pp. 568-576.

[34] Monjezi, M., Shahriar, K., Dehghani, H., & Namin, F. S. (2009). Environmental impact assessment of open pit mining in Iran. Environmental Geology, vol. 58, pp. 205–216.

[35] Rooki, R., Ardejani, F. D., Aryafar, A., & Asadi, A. B. (2011). Prediction of heavy metals in acid mine drainage using artificial neural network from the Shur River of the Sarcheshmeh porphyry copper mine, Southeast Iran. Environmental earth sciences, vol. 64, pp. 1303-1316.

[36] Aryafar, A., Gholami, R., Rooki, R., & Ardejani, F. D. (2012). Heavy metal pollution assessment using support vector machine in the Shur River, Sarcheshmeh copper mine, Iran. Environmental earth sciences, vol. 67, pp. 1191-1199.

[37] Catalão, J. P. d. S., Mariano, S. J. P. S., Mendes, V., & Ferreira, L. (2007). Short-term electricity prices forecasting in a competitive market: A neural network approach. Electric Power Systems Research, vol. 77, pp. 1297-1304.

[38] Shoorehdeli, M. A., Teshnehlab, M., Sedigh, A. K., & Khanesar, M. A. (2009). Identification using ANFIS with intelligent hybrid stable learning algorithm approaches and stability analysis of training methods. Applied Soft Computing, vol. 9, pp. 833-850.

[39] Pousinho, H. M. I., Mendes, V. M. F., & Catalão, J. P. d. S. (2012). Short-term electricity prices forecasting in a competitive market by a hybrid PSO–ANFIS approach. International Journal of Electrical Power & Energy Systems, vol. 39, pp. 29-35.

[40] Rodriguez, C. P., & Anders, G. J. (2004). Energy price forecasting in the Ontario competitive power system market. IEEE transactions on power systems, vol. 19, pp. 366-374.

[41] Heidarian, M., Jalalifar, H., & Rafati, F. (2016). Prediction of rock strength parameters for an Iranian oil field using neuro-fuzzy method. Journal of AI and Data Mining, vol. 4, pp. 229-234.

[42] Zhou, Q. Q., Purvis, M., & Kasabov, N. (1997) A membership function selection method for fuzzy neural networks. In: Proc ICONIP, 1997. pp 785-788.

[43] Jang, J. S. R. (1993). ANFIS: Adaptive-network-based fuzzy inference system. IEEE Transactions on Systems, Man and Cybernetics, vol. 23, pp. 665-685.

[44] Li, H., Chen, C. P., & Huang, H.-P. (2000) Fuzzy neural intelligent systems: Mathematical foundation and the applications in engineering. CRC Press,

[45] Benmiloud, T. Multi-output adaptive neuro-fuzzy inference system. In: wseas international conference on neural networks, 2010. pp 94-98

[46] Tsoukalas, L. H., & Uhrig, R. E. (1996) Fuzzy and neural approaches in engineering. John Wiley & Sons, Inc.

[47] Fattahi, H. Indirect estimation of deformation modulus of an in situ rock mass: an ANFIS model based on grid partitioning, fuzzy c-means clustering

and subtractive clustering. Geosciences Journal, pp. 1-10.

[48] Chiu, S. L. (1994). Fuzzy model identification based on cluster estimation. Journal of intelligent and Fuzzy systems, vol. 2, pp. 267-278.

[49] Stavroulakis, P. (2004) Neuro-fuzzy and Fuzzy-neural Applications in Telecommunications (Signals and Communication Technology). Springer.

[50] Jang, J.-S. R., Sun, C.-T., & Mizutani, E. (1997). Neuro-fuzzy and soft computing-a computational approach to learning and machine intelligence [Book Review]. IEEE Transactions on Automatic Control, vol. 42, pp. 1482-1484.

[51] Chopra, S., Mitra, R., & Kumar, V. (2006). Reduction of fuzzy rules and membership functions and its application to fuzzy PI and PD type controllers. International Journal of Control, Automation and Systems, vol. 4, pp. 438.

[52] Fattahi, H., Shojaee, S., Farsangi, M. A. E., & Mansouri, H. (2013). Hybrid Monte Carlo simulation and ANFIS-subtractive clustering method for reliability analysis of the excavation damaged zone in underground spaces. Computers and Geotechnics, vol. 54, pp. 210-221.

[53] Karimpouli, S., & Fattahi, H. (2016). Estimation of P-and S-wave impedances using Bayesian inversion and adaptive neuro-fuzzy inference system from a carbonate reservoir in Iran. Neural Computing and Applications, pp. 1-14.

[54] Fattahi, H., & Karimpouli, S. (2016). Prediction of porosity and water saturation using pre-stack seismic attributes: a comparison of Bayesian inversion and computational intelligence methods. Computational Geosciences, pp. 1-20.

[55] Fattahi, H. (2017). Prediction of slope stability using adaptive neuro-fuzzy inference system based on clustering methods. Journal of Mining and Environment, vol. 8, pp. 163-177.

[56] Fattahi, H., Nazari, H., & Molaghab, A. (2016). Hybrid ANFIS with ant colony optimization algorithm for prediction of shear wave velocity from a carbonate reservoir in Iran. Int Journal of Mining & Geo-Engineering, vol. 50, pp. 231-238.

[57] Bezdek, J. C. (1973) Fuzzy mathematics in pattern classification. Cornell university, Ithaca

[58] Fattahi, H. (2016). Adaptive neuro fuzzy inference system based on fuzzy C–means clustering algorithm, a technique for estimation of TBM peneteration rate. Int J Optim Civil Eng, vol. 6, pp. 159-171.

نشریه هوش مصنوعی و داده کاوی

سیستم استنتاج عصبی-فازی تطبیقی چند خروجی برای پیش‌بینی آلودگی عناصر سنگین در پساب اسیدی معدنی-مطالعه موردی

هادی فتاحی*، آزاده آگاه و نونا سلیمانپور مقدم

دانشکده مهندسی معدن، دانشگاه صنعتی اراک، اراک، ایران.

ارسال۲۰۱۶/۰۲/۰۷؛ بازنگری ۲۰۱۷/۰۳/۰۵؛ پذیرش ۲۰۱۷/۰۶/۲۷

چکیده:

پساب اسیدی معدنی که مربوط به فعالیت‌های استخراج معدن و مناطقی که دارای دمپ‌های باطله غنی از سولفید هست، مهم‌ترین نگرانی زیست محیطی به حساب می‌آید. تخمین فلزات سنگین در پساب‌های اسیدی یک کار بزرگ در عملیات اصلاحی است. در این مطالعه، یک سیستم استنتاج عصبی فازی تطبیقی چند خروجی برای مدل‌سازی از فلزات سنگین در پساب اسیدی معدنی از مس سرچشمه مورد استفاده قرار گرفته است. هدف از این مطالعه برآورد غلظت مس و آهن، منگنز، روی از پساب اسیدی معدن با استفاده از سیستم استنتاج عصبی فازی تطبیقی چند خروجی با در نظر گرفتن pH و سولفات (SO4) و منیزیم (Mg) در رودخانه شور، مس سرچشمه، جنوب شرقی ایران است. سه مدل سیستم استنتاج عصبی فازی تطبیقی چند خروجی شامل پارتیشن‌بندی شبکه، خوشه‌بندی کاهشی و خوشه بندی C-means فازی در این مطالعه مورد استفاده قرار گرفت. نتایج بدست آمده نشان می‌دهد که روش سیستم استنتاج عصبی فازی تطبیقی چند خروجی- خوشه‌بندی کاهشی (در مقایسه با دو مدل دیگر) یک روش دقیق و با کارایی بالا در پیش‌بینی فلزات سنگین است.

کلمات کلیدی: پساب اسیدی معدن، سیستم استنتاج عصبی-فازی تطبیقی چندخروجی، پارتیشن‌بندی شبکه، خوشه‌بندی کاهشی و خوشه بندی C-means فازی.